



INverse Problem of Identifying a Time-Dependent Coefficient and Free Boundary in Heat Conduction Equation by Using the Meshless Local Petrov-Galerkin (MLPG) Method via Moving Least Squares Approximation

Akbar Karami^a, Saeid Abbasbandy^{a,*}, Elyas Shivanian^a

^aDepartment of Applied Mathematics, Faculty of Science, Imam Khomeini International University, Qazvin, 34149-16818, Iran

Abstract. In this paper we investigated the inverse problem of identifying an unknown time-dependent coefficient and free boundary in heat conduction equation. By using the change of variable we reduced the free boundary problem into a fixed boundary problem. In direct solver problem we employed the meshless local Petrov-Galerkin (MLPG) method based on the moving least squares (MLS) approximation. Inverse reduced problem with fixed boundary is nonlinear and we formulated it as a nonlinear least-squares minimization of a scalar objective function. Minimization is performed by using of *fmincon* routine from MATLAB optimization toolbox accomplished with the *Interior – point* algorithm. In order to deal with the time derivatives, a two-step time discretization method is used. It is shown that the proposed method is accurate and stable even under a large measurement noise through several numerical experiments.

1. Introduction

Many practical problems, such as heat conduction problems are such that they can be modeled as a free boundary problems (FBPs), therefore FBPs have an important role in analyzing engineering science problems and, in general, real world problems. FBPs are boundary-value problems which are defined in a domain, a part of whose boundary is not known at the outset of the problem, that part of the boundary is called a free boundary. The Stefan problem is one kind of the free boundary problems which, describing the process of melting and solidification. In [13, 43] heat conduction fundamentals and in [18, 26, 41, 47] framework of the Stefan free boundary problems are considered. A Free boundary problem can be appear as an inverse coefficients and free boundary identification problem with one or several unknown coefficients. These inverse problems are some of the complex and practical problems that have a great application in engineering science and industry.

In recent years, several methods have been employed for solving the inverse problem of heat conduction equation and Stefan problems numerically, such as the homotopy analysis method [27, 42, 48], Lie-group shooting method [36], finite difference method and finite element method [56] and variational iteration

2010 *Mathematics Subject Classification.* Primary 65M32; Secondary 35R35.

Keywords. Inverse problem, Free boundary, Meshless local Petrov-Galerkin method, Moving least squares, Optimization

Received: 31 October 2019; Revised: 09 February 2020; Accepted: 06 June 2020

Communicated by Marko Nedeljkov

Corresponding author: Saeid Abbasbandy, Tel.: +989121305326.

Email addresses: karami_96@yahoo.com (Akbar Karami), abbasbandy@ikiu.ac.ir, abbasbandy@yahoo.com (Saeid Abbasbandy), shivanian@sci.ikiu.ac.ir (Elyas Shivanian)

method [51]. Grzymkowski and Slota [23, 24] investigated the direct and inverse one-phase Stefan problems by applying the Adomian decomposition method (ADM), and Slota [52] used the homotopy perturbation method for one-phase inverse Stefan problem. In [33] a method of fundamental solutions is applied for the one-dimensional Stefan problem by Johansson et al. In [29–31] inverse Stefan problems of determination time-dependent coefficients and free boundary by using of finite difference method and optimization tools are considered. Determination of a time-dependent free boundary in a two-dimensional parabolic problem was studied in [28]. In [40] the inverse moving boundary problem was solved by applying the radial basis function (RBF) collocation method. The complex variable reproducing kernel particle method and finite point method are applied for inverse problem of heat conduction equations in one dimensional and two dimensional in [16, 17, 53].

For many years, the finite element method (FEM) has been considered as a standard and effective technique for numerically solving many applied problems in Science and engineering. Due to several limitations, this technique alone can not solve some of the complex problems of today's world. For this reason, the development and formulation of new and effective numerical techniques in recent years has been a interesting field of some engineers and mathematicians. In recent years meshless methods have gained considerable attention, as an extension of the numerical methods, in engineering and applied mathematics. Flexibility and simplicity are the advantages of these methods. Meshless methods are presented to overcome the shortcomings of the mesh-based technique, in last decades [39].

Meshless methods are generally divided into three categories. The first category includes methods that use integration and are based on weak forms of PDEs, such as the element free Galerkin method [11, 12, 45, 46, 58]. The second methods are based on the strong forms of PDEs and do not use integration, for example the meshless collocation method based on radial basis functions (RBFs), [1, 2, 22, 34] are in this category, and third category is a set of methods based on the combination of weak forms and strong forms. Implementation of these methods are usually simple, in addition they are also computationally efficient. In spite of several advantages of mentioned methods they also have significant shortcomings, such as numerical instability and less accuracy.

The meshless weak form methods are those that use the global or local weak form. Good stability and excellent accuracy of these methods make them more attractive. In methods that use the global weak form, numerical integrations are carried out on the global background cells in solving the algebraic equations, while in meshless local weak form methods, it does not require any background integration cells for field nodes. The meshless local Petrov-Galerkin (MLPG) method is one of the methods based on the local weak form of PDEs. This method, was first proposed in [6], and later discussed in depth in [4, 5]. In the MLPG method, the numerical integrations are performed over a local small sub-domain defined for each node. The local sub-domains usually have a regular shape, such as interval, circle, square, sphere, cube, etc. Some applications of MLPG method can be found in [3, 6–9, 20, 21, 25], also the several development of the MLPG method for inverse problems of heat conduction equation in recent years can be seen in [35, 49, 50, 57].

The MLS approximation plays an important role in those meshless methods which are based on weak forms such as the element free Galerkin (EFG) method and meshless local Petrov–Galerkin (MLPG) method. By considering a local sub-domain for each field node, the MLS approximates the solving function at each field node. The MLS approximation was developed from the conventional least-squares method and in practical numerical processes, it essentially involves the application of the conventional method to every selected point. A disadvantage of the conventional method is that the final algebraic equations system is sometimes ill-conditioned. The improved moving least-squares (IMLS) approximation was presented by Liew et al. [59]. In the IMLS approximation, the algebra equations system is not ill-condition, and can be solved without obtaining the inverse matrix. Based on the IMLS approximation and the EFG method, an improved element-free Galerkin (IEFG) method has been created [19, 59]. However, the MLS and IMLS approximations are approximations of scalar functions, and thus the meshless method that is derived from them requires a lot of nodes in the domain. The complex variable moving least-squares (CVMLS) [45] and the improved complex variable moving least-squares (ICVMLS) approximations, which are approximation of a vector function, have been developed. Therefore, based on these approximations, the complex variable element-free Galerkin (CVEFG) and the improved complex variable element-free Galerkin (ICVEFG) methods have been presented [10, 14, 15, 37, 38, 44, 54, 55].

The layout of the paper is as follows. In section 2, the formulation of the problem is presented. We briefly describe the MLS approximation in Section 3. Solution of direct problem is considered in Section 4. In this section the time discretization of the problem, the local weak form formulation of the discretized problem, the MLPG discretization of the problem and an example to test the direct solver are presented. We introduce the statement of the inverse problem in section 5. In this section with two examples, the usefulness and effectiveness of the proposed method can be seen. At last, we give a conclusion in Section 6.

2. Statement of the problem

Consider the following heat conduction equation

$$\frac{\partial v(y, t)}{\partial t} = a(t) \frac{\partial^2 v(y, t)}{\partial y^2} + f(y, t), \quad 0 < y < s(t), \quad 0 < t < T < \infty, \quad (1)$$

subject to the initial condition

$$v(y, 0) = \varphi(y), \quad 0 \leq y \leq s_0, \quad s_0 = s(0), \quad (2)$$

and boundary conditions

$$v(0, t) = \mu_1(t), \quad v(s(t), t) = \mu_2(t), \quad 0 \leq t \leq T. \quad (3)$$

In order to determine the unknown coefficient $a(t)$ and free boundary boundary $s(t)$, we impose the over-determination conditions

$$-a(t)v_y(0, t) = \mu_3(t), \quad \int_0^{s(t)} v(y, t) dy = \mu_4(t), \quad 0 \leq t \leq T, \quad (4)$$

where $v(y, t)$, $s(t)$ and $a(t)$ denote the temperature distribution, free boundary and time-dependent thermal diffusivity and $f(y, t)$ is source function. Note that $\mu_2(t)$ and $\mu_3(t)$ represent Cauchy data at the boundary end $x = 0$, while $\mu_4(t)$ represents the specification of the energy of the heat conducting system.

By using the change of variable we reduce the free boundary problem into a fixed boundary problem as follows. Let

$$x = \frac{y}{s(t)}, \quad v(y, t) = v(xs(t), t) = u(x, t), \quad (5)$$

therefore, the following equations are obtained from Eqs. (1) - (4)

$$\frac{\partial u(x, t)}{\partial t} = a(t) \frac{1}{s^2(t)} \frac{\partial^2 u(x, t)}{\partial x^2} + x \frac{s'(t)}{s(t)} \frac{\partial u(x, t)}{\partial x}, \quad 0 < x < 1, \quad 0 < t < T < \infty, \quad (6)$$

$$u(x, 0) = \varphi(s_0 x), \quad 0 \leq x \leq 1, \quad (7)$$

$$u(0, t) = \mu_1(t), \quad u(1, t) = \mu_2(t), \quad 0 \leq t \leq T, \quad (8)$$

$$-a(t)u_x(0, t) = \mu_3(t)s(t), \quad s(t) \int_0^1 u(x, t) dx = \mu_4(t), \quad 0 \leq t \leq T. \quad (9)$$

This problem has been investigated in [30] and [32]. Existence and uniqueness theorems of solution are presented in [32].

In this paper we apply a kind of MLPG method which is based on the Galerkin weak form and moving least squares (MLS) approximation on the Eq. (6), which is subjected to the initial condition (7) and over-specified boundary conditions in Eqs. (8)-(9). Direct problem consist of determination of the temperature distribution $u(x, t)$ together with $\mu_3(t)$ and $\mu_4(t)$, whereas in inverse problem $s(t)$, $a(t)$ and $u(x, t)$ are functions to be determined.

3. The MLS approximation scheme

In this work we used the MLS approximation to represent the trial function at each node. In this section the formulation of MLS approximation has been explained. Consider the sub-domain Ω_s , with the boundary $\partial\Omega_s$, of problem global domain Ω around point x . In fact Ω_s is the domain of definition (or support) of the MLS approximation for the trial function at x . Let $\mathbf{q}^T(x) = [q_1(x), q_2(x), \dots, q_m(x)]$ be a complete monomial basis in the space coordinate x . For example, for one-dimensional case the linear basis is

$$\mathbf{q}^T(x) = [1, x], \quad m = 2, \tag{10}$$

the quadratic basis is

$$\mathbf{q}^T(x) = [1, x, x^2], \quad m = 3, \tag{11}$$

and the cubic basis is

$$\mathbf{q}^T(x) = [1, x, x^2, x^3], \quad m = 4. \tag{12}$$

For all x belong to Ω_s the MLS approximation $u^h(x)$ of u in Ω_s , over a set of random nodes x_i ($i = 1, 2, \dots, n$) located in Ω_s , is given as

$$u^h(x) = \mathbf{q}^T(x)\lambda(x) \quad \forall x \in \Omega_s, \tag{13}$$

where $\lambda^T(x) = [\lambda_1(x), \lambda_2(x), \dots, \lambda_m(x)]$ is a vector of coefficients $q_j(x)$ ($j = 1, 2, \dots, m$). In order to determine the unknown coefficient vector $\lambda(x)$, we define a function $J(\lambda(x))$ as follows

$$J(\lambda(x)) = \sum_{i=1}^n w_i(x)[q^T(x_i)\lambda(x) - \hat{u}_i]^2 = [\mathbf{Q}\lambda(x) - \hat{\mathbf{u}}]^T \mathbf{W}(x)[\mathbf{Q}\lambda(x) - \hat{\mathbf{u}}], \tag{14}$$

where the matrices \mathbf{Q} and $\mathbf{W}(x)$ in Eq. (14) are defined as

$$\mathbf{Q} = \begin{pmatrix} \mathbf{q}^T(x_1) \\ \mathbf{q}^T(x_2) \\ \vdots \\ \mathbf{q}^T(x_n) \end{pmatrix}_{n \times m}, \quad \mathbf{W}(x) = \begin{pmatrix} w_1(x) & \cdots & 0 \\ \vdots & \ddots & \vdots \\ 0 & \cdots & w_n(x) \end{pmatrix}.$$

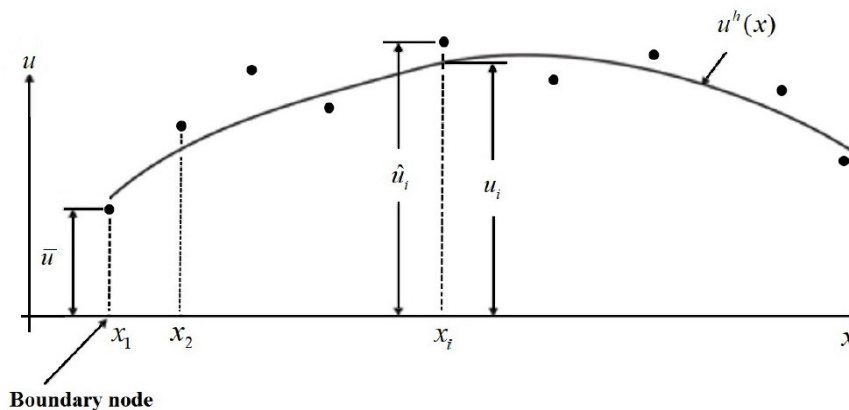


Fig. 1: The distinction between the nodal values u_i of the trial function $u^h(x)$, and the undetermined fictitious nodal values \hat{u}_i .

In the above relations $w_i(x)$, $i = 1, 2, \dots, n$, is the weight function corresponding to the node x_i , so that for each x in the support of $w_i(x)$ we have $w_i(x) > 0$, n is the number of nodes in Ω_s for which the weight functions $w_i(x) > 0$ and $\hat{\mathbf{u}}^T = [\hat{u}_1, \hat{u}_2, \dots, \hat{u}_n]$ is the vector of fictitious nodal values. It is necessary to mention that \hat{u}_i , $i = 1, 2, \dots, n$, are not equal to nodal values u_i , $i = 1, 2, \dots, n$, of the unknown trial function $u^h(x)$ in general (Fig. 1). The stationarity of $J(\lambda(x))$ in Eq. (14) with respect to $\lambda(x)$ the following matrix equation is obtained:

$$\mathbf{F}(x)\lambda(x) = \mathbf{G}(x)\hat{\mathbf{u}}, \tag{15}$$

where $\mathbf{F}(x)$ and $\mathbf{G}(x)$ are matrices defined as follows

$$\mathbf{F}(x) = \mathbf{Q}^T \mathbf{W}(x) \mathbf{Q} = \mathbf{G}(x) \mathbf{Q} = \sum_{i=1}^n w_i(x) \mathbf{q}(x_i) \mathbf{q}^T(x_i), \tag{16}$$

$$\mathbf{G}(x) = \mathbf{Q}^T \mathbf{W}(x) = [w_1(x) \mathbf{q}(x_1), w_2(x) \mathbf{q}(x_2), \dots, w_n(x) \mathbf{q}(x_n)]. \tag{17}$$

The MLS approximation is well-defined only when the matrix \mathbf{F} in Eq. (15) is non-singular, i.e. if and only if the rank of \mathbf{Q} equals m . A necessary condition to have a well-defined MLS approximation is that at least m weight functions are non-zero (i.e. $n > m$) for each sample point $x \in \Omega$. Computing $\lambda(x)$ from Eq. (15) and substituting it into Eq. (13), gives

$$u^h(x) = \Phi^T(x) \cdot \hat{\mathbf{u}} = \sum_{i=1}^n \phi_i(x) \hat{u}_i, \quad x \in \Omega_s, \tag{18}$$

where

$$\Phi^T(x) = \mathbf{q}^T(x) \mathbf{F}^{-1}(x) \mathbf{G}(x), \tag{19}$$

or

$$\phi_i(x) = \sum_{j=1}^m q_j(x) [\mathbf{F}^{-1}(x) \mathbf{G}(x)]_{ji}. \tag{20}$$

The function ϕ_i is usually called the shape function of the MLS approximation corresponding to nodal point x_i . The partial derivative of $\phi_i(x)$ with respect to x is defined as

$$\phi_{i,x} = \sum_{j=1}^m [q_{j,x} (\mathbf{F}^{-1} \mathbf{G})_{ji} + q_j (\mathbf{F}^{-1} \mathbf{G}_{,x} + \mathbf{F}_{,x}^{-1} \mathbf{G})_{ji}], \tag{21}$$

in which $(\mathbf{F}^{-1})_{,x} = \mathbf{F}_{,x}^{-1} = -\mathbf{F}^{-1} \mathbf{F}_{,x} \mathbf{F}^{-1}$ and $(\cdot)_{,x}$ denotes the derivative with respect to x . In this paper the Gaussian weight function is used that defined as

$$w_i(x) = \begin{cases} \frac{\exp[-(\frac{l_i}{c_i})^2] - \exp[-(\frac{r_s}{c_i})^2]}{1 - \exp[-(\frac{r_s}{c_i})^2]}, & 0 \leq l_i \leq r_s, \\ 0, & l_i \geq r_s, \end{cases}$$

where $l_i = \|x - x_i\|$, c_i is a constant controlling the shape of the weight function $w_i(x)$ and r_s is the size of the support domain. r_s must be chosen large enough to have sufficiently number of nodes covered in the domain of definition of every sample point ($n \geq m$) to ensure the regularity of \mathbf{F} .

4. Solution of direct problem

4.1. The time discretization approximation

In this work the following finite difference approximation is used to approximate the time derivative

$$\frac{\partial u(x,t)}{\partial t} \cong \frac{1}{\Delta t} (u^{k+1}(x) - u^k(x)), \tag{22}$$

where $u^j(x) = u(x, t_j)$, $s^j = s(t_j)$, $t_0 = 0$, $t_j = t_0 + j\Delta t$, $j = 0, 1, \dots, M$ and $\Delta t = \frac{T}{M}$. Also by using the Crank-Nicolson technique we have the following approximations:

$$\frac{a(t)}{s^2(t)} \frac{\partial^2 u(x,t)}{\partial x^2} \cong \frac{1}{2} \left(\frac{a^{k+1}}{(s^{k+1})^2} u_{xx}^{k+1} + \frac{a^k}{(s^k)^2} u_{xx}^k \right), \tag{23}$$

$$\frac{s'(t)}{s(t)} \frac{\partial u(x,t)}{\partial x} \cong \frac{1}{2} \left(\frac{s'^{k+1}}{s^{k+1}} u_x^{k+1} + \frac{s'^k}{s^k} u_x^k \right), \tag{24}$$

$$f(xs(t), t) \cong \frac{1}{2} (f^{k+1} + f^k), \tag{25}$$

where $f^{(j)} = f(xs^j, t_j)$. Considering the above approximations, Eq. (6) can be written as:

$$\frac{u^{k+1} - u^k}{\Delta t} = \frac{1}{2} \left(\frac{a^{k+1}}{(s^{k+1})^2} u_{xx}^{k+1} + \frac{a^k}{(s^k)^2} u_{xx}^k \right) + \frac{x}{2} \left(\frac{s'^{k+1}}{s^{k+1}} u_x^{k+1} + \frac{s'^k}{s^k} u_x^k \right) + \frac{1}{2} (f^{k+1} + f^k). \tag{26}$$

Suppose that $\lambda = \frac{2}{\Delta t}$, then we have

$$\lambda u^{k+1} - x \frac{s'^{k+1}}{s^{k+1}} u_x^{k+1} - \frac{a^{k+1}}{(s^{k+1})^2} u_{xx}^{k+1} = \lambda u^k + x \frac{s'^k}{s^k} u_x^k + \frac{a^k}{(s^k)^2} u_{xx}^k + (f^{k+1} + f^k). \tag{27}$$

4.2. The meshless local weak form formulation

Let Ω_q^i be a sub-domain associated with the nodal point x_i , $i = 1, 2, \dots, N$, (called local quadrature cell) in the global domain Ω . Ω_q^i , $i = 1, 2, \dots, N$, overlap each other and union of them cover the whole global domain Ω . In this paper Ω_q^i are intervals centered at x_i of radius r_q . By applying the MLPG method, the local weak form is obtained over local quadrature cells Ω_q^i . For each node $x_i \in \Omega_q^i$ the local weak of Eq. (27) is represented as follows

$$\begin{aligned} &\lambda \int_{\Omega_q^i} u^{k+1} v(x) dx - \frac{s'^{k+1}}{s^{k+1}} \int_{\Omega_q^i} x u_x^{k+1} v(x) dx - \frac{a^{k+1}}{(s^{k+1})^2} \int_{\Omega_q^i} u_{xx}^{k+1} v(x) dx = \\ &\lambda \int_{\Omega_q^i} u^k v(x) dx + \frac{s'^k}{s^k} \int_{\Omega_q^i} x u_x^k v(x) dx + \frac{a^k}{(s^k)^2} \int_{\Omega_q^i} u_{xx}^k v(x) dx + \int_{\Omega_q^i} (f^{k+1} + f^k) v(x) dx, \end{aligned} \tag{28}$$

where the Heaviside step function $v(x)$ is used as the test function in Ω_q^i which is defined as

$$v(x) = \begin{cases} 1, & \mathbf{x} \in \Omega_q^i, \\ 0, & \mathbf{x} \notin \Omega_q^i. \end{cases} \tag{29}$$

Using the integration by parts Eq. (28) converts to the following local weak form equation:

$$\begin{aligned} &\lambda \int_{\Omega_q^i} u^{k+1} dx - \frac{s'^{k+1}}{s^{k+1}} \int_{\Omega_q^i} x u_x^{k+1} dx - \frac{a^{k+1}}{(s^{k+1})^2} u_x^{k+1} |_{\partial \Omega_q^i} = \\ &\lambda \int_{\Omega_q^i} u^k dx + \frac{s'^k}{s^k} \int_{\Omega_q^i} x u_x^k dx + \frac{a^k}{(s^k)^2} u_x^k |_{\partial \Omega_q^i} + \int_{\Omega_q^i} (f^{k+1} + f^k) dx, \end{aligned} \tag{30}$$

where $\partial \Omega_q^i$ is the boundary of Ω_q^i .

In the next section by using of MLS approximation for the unknown functions, a system of algebraic equations with unknown quantities is obtained from the local integral equation (30).

4.3. MLPG Discretization

In this section, discretization of the Eq. (30) is desired. For this purpose, we consider the N regularly points $x_i, i = 1, 2, \dots, N$, in the domain of the problem and its boundary such that $x_{i+1} - x_i = h$. Suppose that $u(x_i, t_k)$, is determined and $u(x_i, t_{k+1})$, is unknown for $i = 1, 2, \dots, N$. In order to determine the N unknown quantities $u(x_i, t_{k+1})$ we need to have N equations. For interior nodes x_i of the domain Ω , by replacing MLS approximation formula (18) in the equations (30), the following discrete equations are obtained as

$$\begin{aligned} & \lambda \sum_{j=1}^N \left(\int_{\Omega_q^i} \phi_j(x) dx \right) u_j^{(k+1)} - \frac{s'^{k+1}}{s^{k+1}} \sum_{j=1}^N \left(\int_{\Omega_q^i} x \phi_j'(x) dx \right) u_j^{(k+1)} - \\ & \frac{a^{k+1}}{(s^{k+1})^2} \sum_{j=1}^N \phi_j'(x) u_j^{(k+1)} |_{\partial \Omega_q^i} = \lambda \sum_{j=1}^N \left(\int_{\Omega_q^i} \phi_j(x) dx \right) u_j^{(k)} + \\ & \frac{s'^k}{s^k} \sum_{j=1}^N \left(\int_{\Omega_q^i} x \phi_j'(x) dx \right) u_j^{(k)} + \frac{a^k}{(s^k)^2} \sum_{j=1}^N \phi_j'(x) u_j^{(k)} |_{\partial \Omega_q^i} + F_i^{(k)}, \end{aligned} \tag{31}$$

where

$$F_i^{(k)} = \int_{\Omega_q^i} (f^{k+1} + f^k) dx.$$

For nodes $x = 0$ and $x = 1$ which are located on the boundary of problem, we set

$$u^{k+1}(0) = \mu_1((k + 1)\Delta t), \tag{32}$$

$$u^{k+1}(1) = \mu_2((k + 1)\Delta t). \tag{33}$$

The matrix form of Eqs. (31) for all N nodal points in domain and on boundary of the problem can be represented as follows

$$\begin{aligned} & \left[\lambda \sum_{j=1}^N a_{ij} - \frac{s'^{k+1}}{s^{k+1}} \sum_{j=1}^N b_{ij} - \frac{a^{k+1}}{(s^{k+1})^2} \sum_{j=1}^N c_{ij} \right] u_j^{(k+1)} = \\ & \left[\lambda \sum_{j=1}^N a_{ij} + \frac{s'^k}{s^k} \sum_{j=1}^N b_{ij} + \frac{a^k}{(s^k)^2} \sum_{j=1}^N c_{ij} \right] u_j^{(k)} + F_i^{(k)}, \end{aligned} \tag{34}$$

where

$$a_{ij} = \int_{\Omega_q^i} \phi_j(x) dx, \quad b_{ij} = \int_{\Omega_q^i} x \phi_j'(x) dx, \quad c_{ij} = \phi_j'(x) |_{\partial \Omega_q^i}. \tag{35}$$

Assuming that

$$A_{ij} = \lambda a_{ij} - \frac{s'^{k+1}}{s^{k+1}} b_{ij} - \frac{a^{k+1}}{(s^{k+1})^2} c_{ij}, \tag{36}$$

$$B_{ij} = \lambda a_{ij} + \frac{s'^k}{s^k} b_{ij} + \frac{a^k}{(s^k)^2} c_{ij}, \tag{37}$$

and $U = (u_i)_{N \times 1}$, Eqs. (34) yield the following system of equations

$$AU^{(k+1)} = BU^{(k)} + F^k. \tag{38}$$

To satisfy Eq. (38), for nodes belong to the boundary, i.e. $x = 0$ and $x = 1$, we set for each step

$$A_{11} = A_{NN} = 1, \quad \forall j \neq 1 : A_{1j} = 0, \quad \forall j \neq N : A_{Nj} = 0,$$

$$B_{11} = B_{NN} = 1, \quad \forall j \neq 1 : B_{1j} = 0, \quad \forall j \neq N : B_{Nj} = 0,$$

$$F_1^k = \mu_1((k + 1)\Delta t), \quad F_N^k = \mu_2((k + 1)\Delta t).$$

At first step, when $k = 0$, according to the initial conditions, we apply the following assumptions:

$$U^{(0)} = [\varphi(s_0x_1), \varphi(s_0x_2), \dots, \varphi(s_0x_N)]^T. \quad (39)$$

4.4. Numerical experiments

In this section we test the described approach for direct problem with an example. We consider the problem (6)-(9) with $T = 1$ and

$$\begin{aligned} s(t) &= 1 + 2t, & a(t) &= 1 + t^2, \\ \mu_1(t) &= 1 + 8t, & \mu_2(t) &= (2 + 2t)^2 + 8t, \\ \varphi(y) &= (1 + y)^2, & f(y, t) &= 6 - 2t^2. \end{aligned}$$

In direct problem $v(y, t)$, $\mu_3(t)$ and $\mu_4(t)$ are functions to be determined. The analytical solution of problem is given by

$$\begin{aligned} v(y, t) &= (1 + y)^2 + 8t, \\ \mu_3(t) &= -(2 + 2t^2), & \mu_4(t) &= \frac{(2 + 2t)^3 - 1}{3} + 8t(1 + 2t), \end{aligned}$$

and

$$\begin{aligned} u(x, t) &= v(xs(t), t) = (1 + x + 2xt)^2 + 8t, \\ \mu_3(t) &= -(2 + 2t^2), & \mu_4(t) &= \frac{(2 + 2t)^3 - 1}{3} + 8t(1 + 2t). \end{aligned}$$

In this example, the domain integrals are approximated using the 4 points Gaussian quadrature rule. In order to investigate the accuracy of computed approximations and the efficiency of the presented method, the following root mean square error (rmse) and absolute error formulas are applied

$$\text{Absolute error}(u(x_i, t_j)) = |u_{\text{exact}}(x_i, t_j) - u_{\text{approx}}(x_i, t_j)|, \quad (40)$$

$$\text{rmse}(\mu(t)) = \sqrt{\frac{\sum_{j=0}^M (\mu_{\text{exact}}(t_j) - \mu_{\text{approx}}(t_j))^2}{M + 1}}. \quad (41)$$

In implementing the meshless local weak form, each local quadrature domain Ω_q^i is taken as interval centered at x_i of radius $r_q = 0.7h$ where $h = x_{i+1} - x_i$, $i = 1, 2, \dots, N$. Also the radius of support domain Ω_s is $r_s = 4r_q$, $c = 1.17h$ and the quadratic basis functions (11) is used in Eq. (13). Fig. 2 and Fig. 3 presents the Exact solution, Numerical solution and Absolute errors for $u(x, t)$ and $v(y, t)$ with $h = \Delta t = 0.025$, and $T = 1$. Exact solution and numerical solution for $\mu_3(t)$ and $\mu_4(t)$ also are plotted in Fig. 4. Table 1 gives the $\text{rmse}(\mu_3(t))$ and $\text{rmse}(\mu_4(t))$ for different values of h and Δt . These have been approximated using the Simpson rule for integration and the following formula for derivatives

$$\frac{\partial u(0, t_j)}{\partial x} \cong \sum_{j=0}^{j=M} \phi'_j(0) u_j^k, \quad (42)$$

where $\phi_i(x)$ is defined in (20). Obtained results show a very good agreement between the exact and numerical solutions.

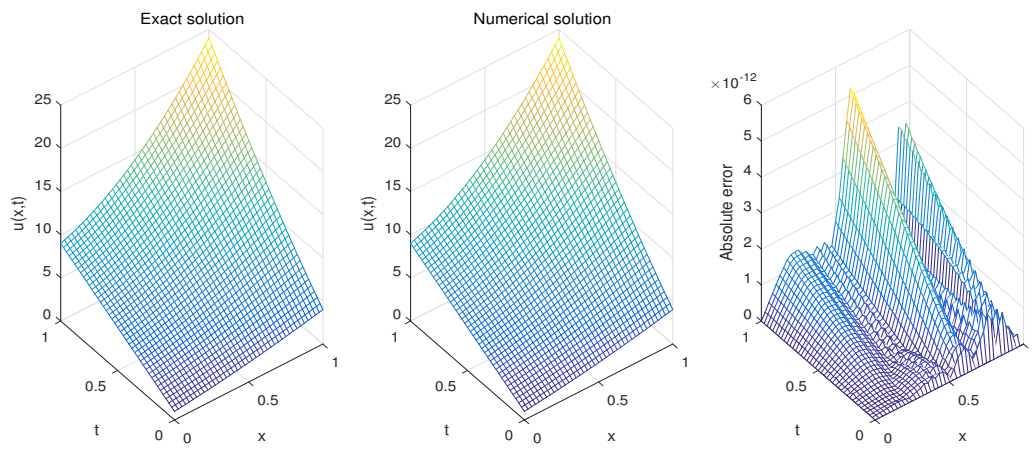


Fig. 2. Diagram of Exact solution, Numerical solution and Absolute error for $u(x, t)$ when $h = \Delta t = 0.025$.

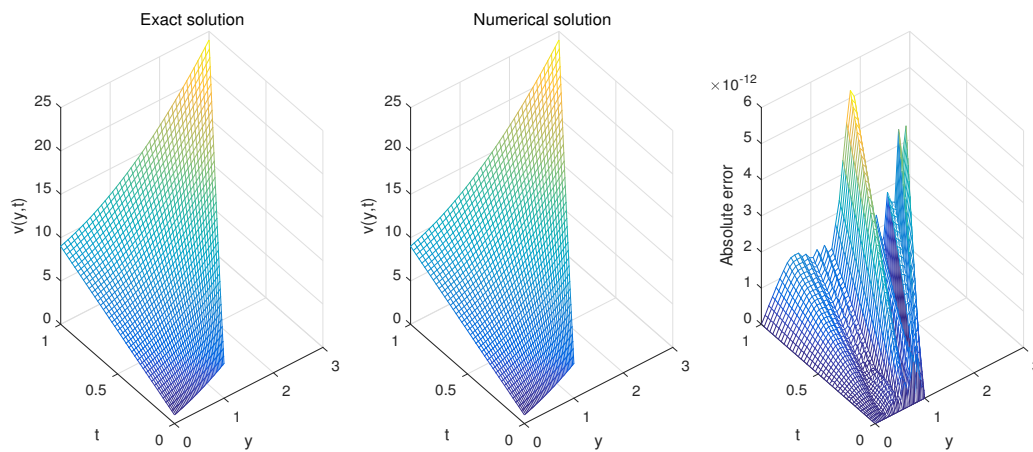


Fig. 3. Diagram of Exact solution, Numerical solution and Absolute error for $v(y, t)$ when $h = \Delta t = 0.025$.

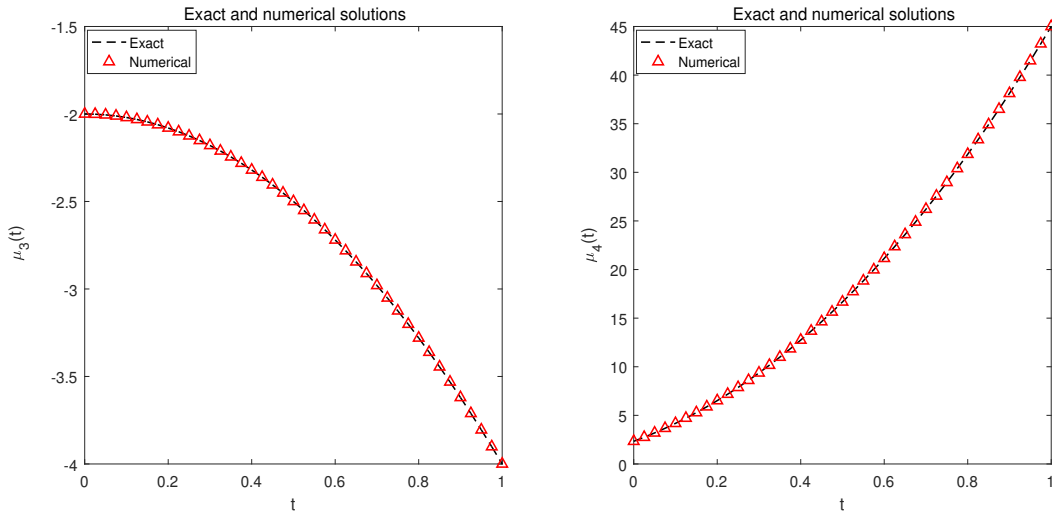


Fig. 4. Diagram of Exact solution and Numerical solutions for $\mu_3(t)$ and $\mu_4(t)$ when $h = \Delta t = 0.025$.

Table 1. The rmse for $\mu_3(t)$ and $\mu_3(t)$ when $h = \Delta t \in \{0.1, 0.05, 0.025, 0.01\}$ in direct problem.

h	$h = \Delta t = 0.1$	$h = \Delta t = 0.05$	$h = \Delta t = 0.025$	$h = \Delta t = 0.01$
$rmse(\mu_3(t))$	$2.008622e - 13$	$2.343945e - 12$	$3.216328e - 12$	$7.840626e - 11$
$rmse(\mu_4(t))$	$1.913527e - 13$	$2.200038e - 12$	$2.224144e - 12$	$4.993713e - 11$

5. Inverse problem

5.1. Statement of the inverse problem

Inverse problem is considered with unknown free boundary, thermal diffusivity and temperature distribution i.e. $s(t)$, $a(t)$ and $u(x, t)$. The inverse problem (6)-(9) is a nonlinear problem and we can formulate it as a nonlinear least-squares minimization problem. The objective function to be minimized is defined as follows

$$E(s, a) = \left\| -\frac{a(t)}{s(t)}u_x(0, t) - \mu_3(t) \right\|_{L^2(0,T)}^2 + \left\| s(t) \int_0^1 u(x, t)dx - \mu_4(t) \right\|_{L^2(0,T)}^2. \tag{43}$$

The discretized form of recent equation is

$$E(\mathbf{s}, \mathbf{a}) = \sum_{j=0}^{j=M} \left[-\frac{a_j}{s_j}u_x(0, t_j) - \mu_3(t_j) \right]^2 + \sum_{j=0}^{j=M} \left[s_j \int_0^1 u(x, t_j)dx - \mu_4(t_j) \right]^2, \tag{44}$$

where $\mathbf{s} = (s_0, s_1, \dots, s_M)$ and $\mathbf{a} = (a_0, a_1, \dots, a_M)$. According to the numerical results obtained in the next section it seems that the problem being rather stable even under a large measurement noise in the input data $\mu_3(t)$ and $\mu_4(t)$ therefore, there is no need to regularize the objective function (43) by adding a Tikhonov penalty term of some norm of $s(t)$ and $a(t)$.

The minimization of nonlinear objective function $E(\mathbf{s}, \mathbf{a})$ with constrains $s_j, a_j > 0$ ($j = 0, 1, \dots, M$) was performed by using the *fmincon* routine MATLAB toolbox accomplished with the *Interior-point* algorithm. The *fmincon* minimizer by starting from an initial guesses tries to find the minimum value of the objective function and minimizer parameters s_j and a_j ($j = 0, 1, \dots, M$). In inverse problem derivatives $u_x(0, t_j)$ are

approximated by Eq. (42) and integrations $\int_0^1 u(x, t_j) dx$ are computed with Trapezoidal rule. Furthermore, when we apply the inverse problem solver, $s'(t_j)$ is approximated by

$$s'(t_j) \cong \frac{s(t_{j+1}) - s(t_j)}{\Delta t}, \tag{45}$$

in direct solver. For implementing the routine *fmincon* we take the interval $(10^{-10}, 10^3)$ as a bound for s_j and a_j . In addition we take other parameters for routine *fmincon* as follow

- Maximum function evaluations= 3000,
- Maximum iterations= 1000,
- Optimality tolerance= 10^{-6} ,
- Step tolerance= 10^{-10} ,
- Constraint tolerance= 10^{-6} .

5.2. Numerical experiments

In this section with two examples we test the approach described for inverse problem. In applications input data $\mu_3(t_j)$ and $\mu_4(t_j)$ are contaminated by noise. In this paper we consider the inverse problem without noise and with random noisy data as follows

$$\tilde{\mu}_3(t_j) = \mu_3(t_j)(1 + \delta R_1(j)), \tag{46}$$

$$\tilde{\mu}_4(t_j) = \mu_4(t_j)(1 + \delta R_2(j)), \quad j = 0, 1, 2, \dots, M, \tag{47}$$

where δ denote the level of noise, and $R_1(j)$ and $R_2(j)$ are random numbers in $[-1, 1]$.

In order to investigate the accuracy of computed approximations and the efficiency of the presented method, we applied the root mean square error (rmse) and Relative error formulas as follows

$$rmse(s(t)) = \sqrt{\frac{\sum_{j=0}^M (s_{exact}(t_j) - s_{approx}(t_j))^2}{M + 1}}, \tag{48}$$

$$rmse(a(t)) = \sqrt{\frac{\sum_{j=0}^M (a_{exact}(t_j) - a_{approx}(t_j))^2}{M + 1}}, \tag{49}$$

$$Relative\ error(u(x_i, t_j)) = \frac{|u_{exact}(x_i, t_j) - u_{approx}(x_i, t_j)|}{|u_{exact}(x_i, t_j)|}. \tag{50}$$

Example 1. Consider the the problem (6)-(9) with

$$\begin{aligned} \mu_1(t) &= 1 + 8t, & \mu_2(t) &= (2 + 2t)^2 + 8t, \\ \mu_3(t) &= -(2 + 2t^2), & \mu_4(t) &= \frac{(2 + 2t)^3 - 1}{3} + 8t(1 + 2t), \\ \varphi(y) &= (1 + y)^2, & f(y, t) &= 6 - 2t^2, \end{aligned}$$

and unknown free boundary $s(t)$ and coefficient $a(t)$. The analytical solutions are given by

$$\begin{aligned} v(y, t) &= (1 + y)^2 + 8t, \\ s(t) &= 1 + 2t, & a(t) &= 1 + t^2, \end{aligned}$$

and

$$\begin{aligned} u(x, t) &= v(xs(t), t) = (1 + x + 2xt)^2 + 8t, \\ s(t) &= 1 + 2t, & a(t) &= 1 + t^2. \end{aligned}$$

The results of using the proposed method are obtained with $h = \Delta t = 0.025$ and $T = 1$. In direct solver, when we solve the inverse problem, each local quadrature domain Ω_q^i is taken as interval centered at x_i of radius $r_q = 0.7h$ where $h = x_{i+1} - x_i$, $i = 1, 2, \dots, N$. Also the radius of support domain Ω_s is $r_s = 4r_q$, $c = 1.17h$ and the quadratic basis functions (11) is used in Eq. (13). The domain integrals in direct solver also are approximated using the 4 points Gaussian quadrature rule. In this example the initial guesses for free boundary and thermal diffusivity at different time steps are $s_j = 1, a_j = 1$ for $j = 0, 1, \dots, M$.

We first consider the case in which there is no noise in $\mu_3(t_j)$ and $\mu_4(t_j)$. In this case, the objective function E as a function of parameters s_j and a_j decreases very fast in small number of iterations. After a few iterations convergence is achieved and objective function takes a stationary values of order 10^{-9} . Diagrams of exact solution and numerical solution for $s(t)$ and $a(t)$ are plotted in Fig. 5. Diagrams of exact solution and numerical solution and relative error for $u(x, t)$ and $v(y, t)$ also are presented in Fig. 6. and Fig. 7. Obtained results for $\delta = 0$ show a very good agreement between the exact and numerical solutions. When the input data $\mu_3(t_j)$ and $\mu_4(t_j)$ contaminate with level noise $\delta = 0.02$ the objective function is again convergence very fast and takes stationary values of order 10^{-7} . Exact solution and numerical solution for $s(t)$, $a(t)$, $u(x, t)$, $v(y, t)$ and relative error for $u(x, t)$ and $v(y, t)$ are presented in Fig. 5., Fig. 8. and Fig. 9. Values of $rmse$ for $s(t)$ and $a(t)$ and values of objective function in last iteration are given in Table 2. From the obtained results it can be seen that the small perturbation in input data does not significantly affect in the output solutions. It can be concluded that approximated solutions are stable.

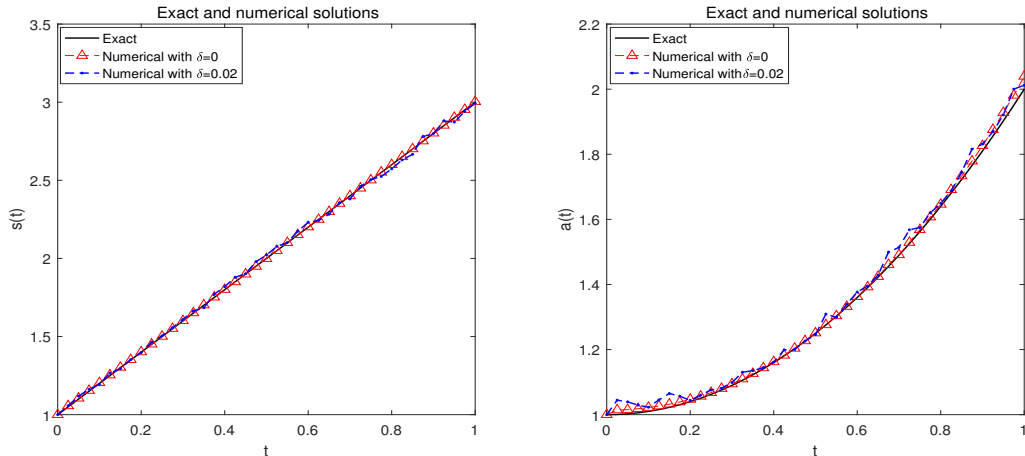


Fig. 5. For example1: Diagram of Exact solution, Numerical solution for $s(t)$ and $a(t)$ without noise ($\delta = 0$) and with $\delta = 0.02$ and $h = \Delta t = 0.025$

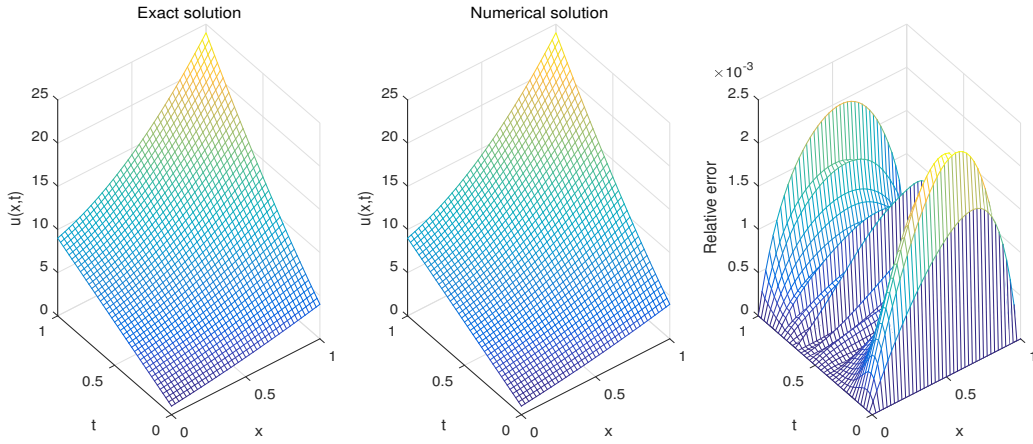


Fig. 6. For Example 1: Diagram of Exact solution, Numerical solution and Relative error for $u(x, t)$ without noise and with $h = \Delta t = 0.025$.

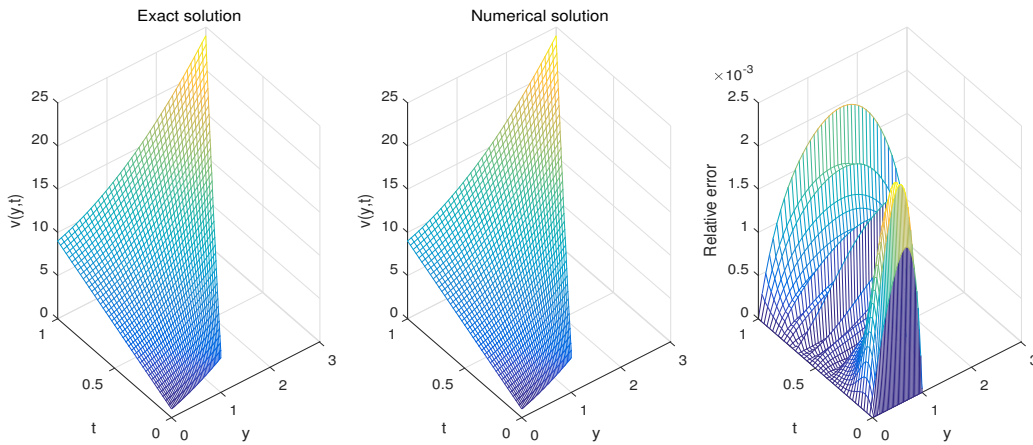


Fig. 7. For Example 1: Diagram of Exact solution, Numerical solution and Relative error for $v(x, t)$ without noise and with $h = \Delta t = 0.025$.

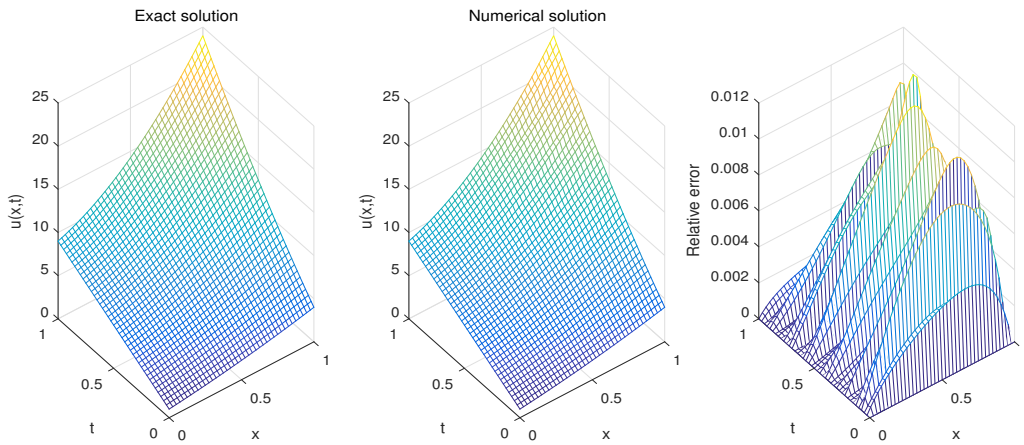


Fig. 8. For Example 1: Diagram of Exact solution, Numerical solution and Relative error for $u(x, t)$ with $\delta = 0.02$ and with $h = \Delta t = 0.025$

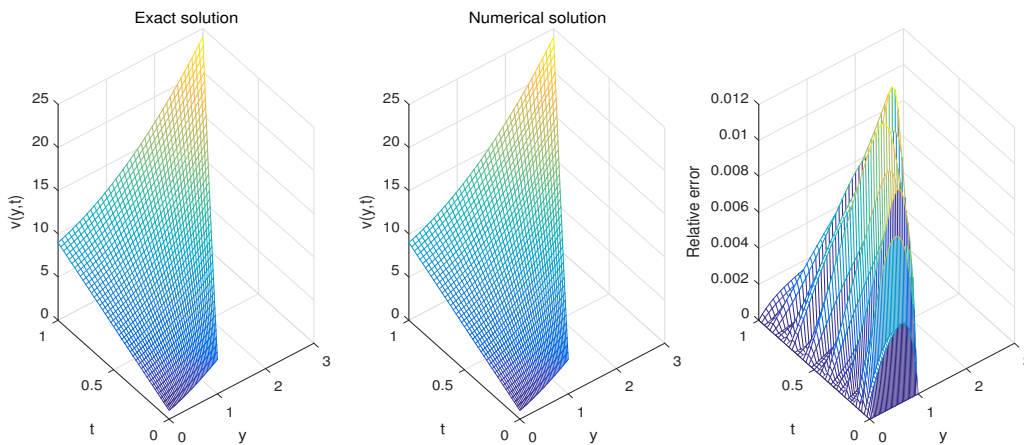


Fig. 9. For Example 1: Diagram of Exact solution, Numerical solution and Relative error for $v(x, t)$ with $\delta = 0.02$ and with $h = \Delta t = 0.025$

Table 2: For Example 1 and Example 2: *rmse* values for $s(t)$ and $a(t)$ and values of objective function at final iterations without noise and with level noise $\delta = 0.02$ when $h = \Delta t = 0.025$

	rmse	$\delta = 0$	$\delta = 0.02$
Example 1	rmse($s(t)$)	0.002243	0.016018
	rmse($a(t)$)	0.011574	0.025649
	Values of objective function at final iteration	$2.230615e - 09$	$6.875563e - 07$
Example 2	rmse($s(t)$)	0.000427	0.010687
	rmse($a(t)$)	0.000540	0.012325
	Values of objective function at final iteration	$6.037903e - 13$	$1.037434e - 11$

Example 2. Consider the the problem (6)-(9) with

$$\begin{aligned} \mu_1(t) &= 1 + 8t, & \mu_2(t) &= (1 + \sqrt{2-t})^2 + 8t, \\ \mu_3(t) &= -2\sqrt{1+t}, & \mu_4(t) &= \frac{(1 + \sqrt{2-t})^3 - 1}{3} + 8t\sqrt{2-t}, \\ \varphi(y) &= (1 + \sqrt{2}y)^2, & f(y, t) &= 8 - 2\sqrt{1+t}. \end{aligned}$$

With this data the analytical solution is given by

$$\begin{aligned} v(y, t) &= (1 + y)^2 + 8t, \\ s(t) &= \sqrt{2-t}, & a(t) &= \sqrt{1+t}, \end{aligned}$$

and

$$\begin{aligned} u(x, t) &= v(xs(t), t) = (1 + x\sqrt{2-t})^2 + 8t, \\ s(t) &= \sqrt{2-t}, & a(t) &= \sqrt{1+t}. \end{aligned}$$

The results of using the proposed method are obtained with $h = \Delta t = 0.025$ and $T = 1$. In direct solver, when we solve the inverse problem, each local quadrature domain Ω_q^i is taken as interval centered at x_i of radius $r_q = 0.7h$ where $h = x_{i+1} - x_i$, $i = 1, 2, \dots, N$. Also the radius of support domain Ω_s is $r_s = 4r_q$, $c = 1.17h$ and the quadratic basis functions (11) is used in Eq. (13). The domain integrals in direct solver also are approximated using the 4 points Gaussian quadrature rule. In this example the initial guesses for free boundary and thermal diffusivity at different time steps are $s_j = 1, a_j = 1$ for $j = 0, 1, \dots, M$.

We first consider the case in which there is no noise in $\mu_3(t_j)$ and $\mu_4(t_j)$. In this case, the objective function E as a function of parameters s_j and a_j decreases very fast in small number of iterations. The objective function takes a stationary values of order 10^{-13} at the final iteration. Diagrams of exact solution and numerical solution for $s(t)$ and $a(t)$ are plotted in Fig. 10. Diagrams of exact solution and numerical solution and relative error for $u(x, t)$ and $v(y, t)$ also are presented in Fig. 11. and Fig. 12. Obtained results for $\delta = 0$ show a very good agreement between the exact and numerical solutions. When the input data $\mu_3(t_j)$ and $\mu_4(t_j)$ are contaminate with level noise $\delta = 0.02$ the objective function is again convergence very fast and takes stationary values of order 10^{-11} at the final iteration. Exact solution and numerical solution for $s(t)$, $a(t)$, $u(x, t)$, $v(y, t)$ and relative error for $u(x, t)$ and $v(y, t)$ are presented in Fig. 10., Fig. 13. and Fig. 14. Values of $rmse$ for $s(t)$ and $a(t)$ and values of objective function in last iteration are given in Table 2. From the obtained results it can be seen that the small perturbation in input data does not significantly affect in the output solutions. It can be concluded in this example also that approximated solutions are stable.

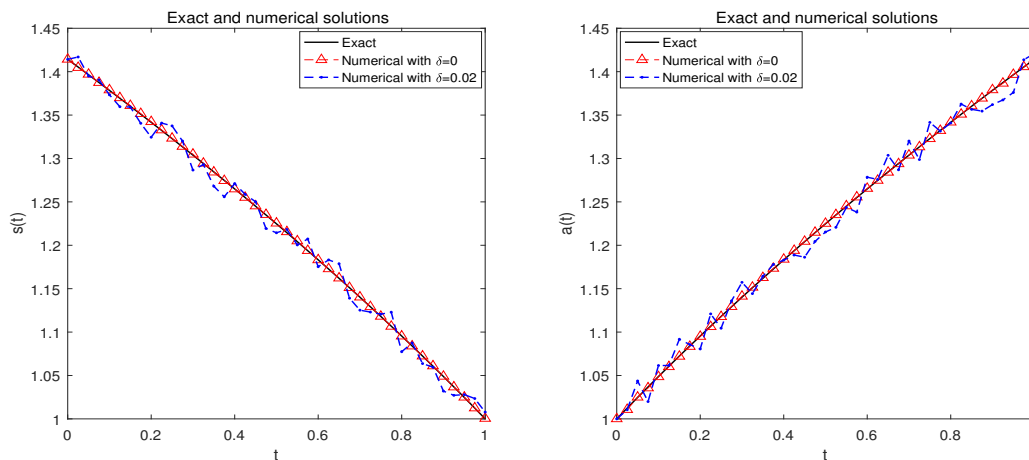


Fig. 10. For Example 2: Diagram of Exact solution, Numerical solution for $s(t)$ and $a(t)$ without noise ($\delta = 0$) and with $\delta = 0.02$ and $h = \Delta t = 0.025$

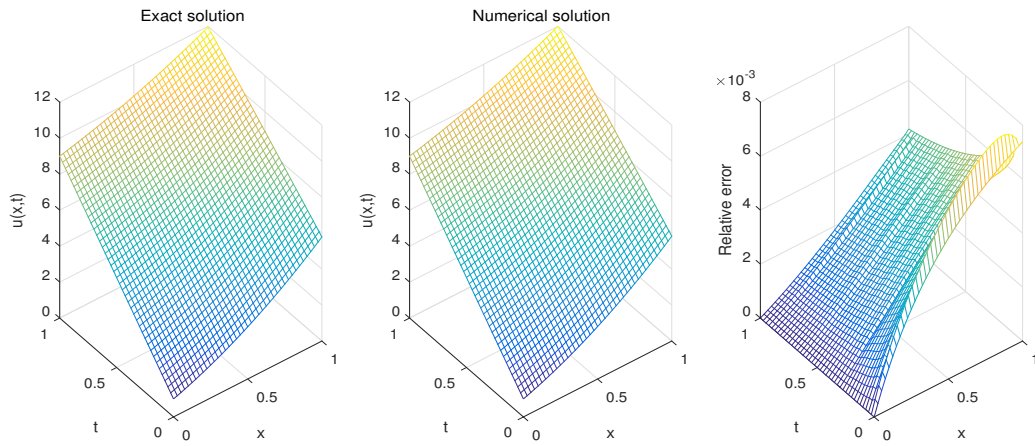


Fig. 11. For Example 2: Diagram of Exact solution, Numerical solution and Relative error for $u(x, t)$ with $\delta = 0$ and with $h = \Delta t = 0.025$

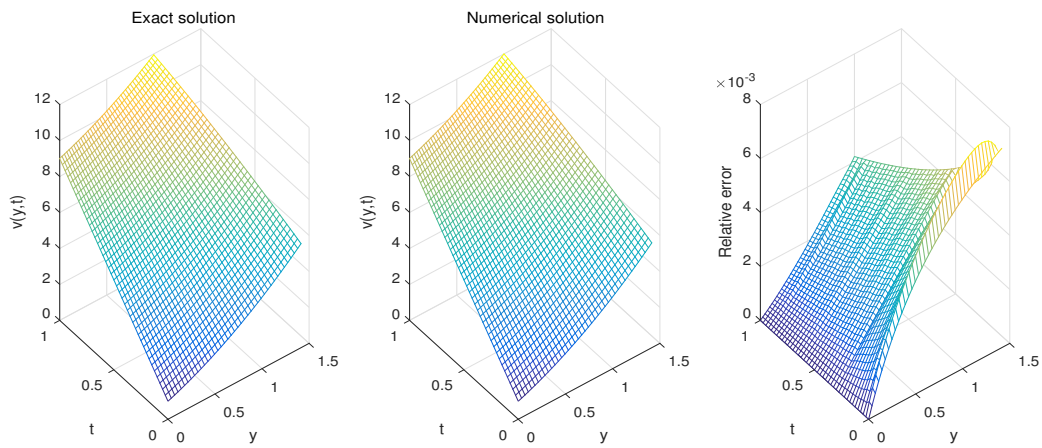


Fig. 12. For Example 2: Diagram of Exact solution, Numerical solution and Relative error for $v(x, t)$ with $\delta = 0$ and with $h = \Delta t = 0.025$

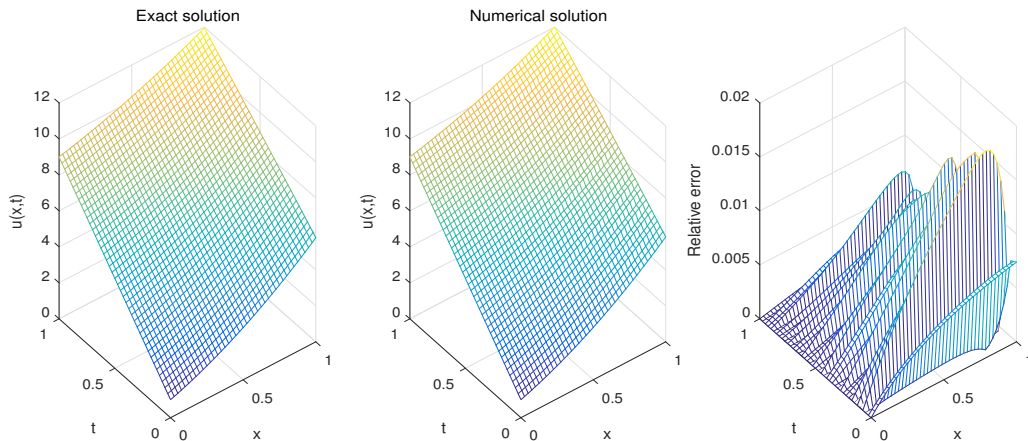


Fig. 13. For Example 2: Diagram of Exact solution, Numerical solution and Relative error for $u(x, t)$ with $\delta = 0.02$ and with $h = \Delta t = 0.025$

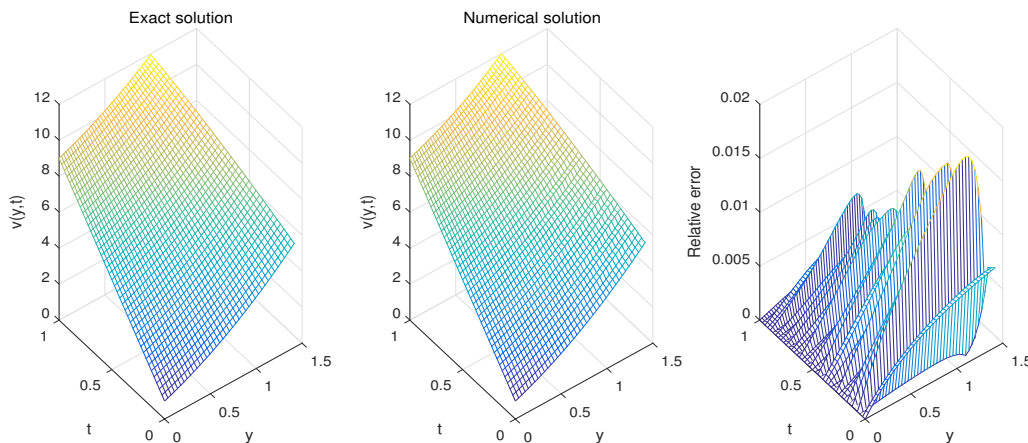


Fig. 14. For Example 2: Diagram of Exact solution, Numerical solution and Relative error for $v(x, t)$ with $\delta = 0.02$ and with $h = \Delta t = 0.025$

6. Conclusions

In this paper, inverse problem of free boundary and coefficient thermal identification is considered. For solving this problem by using the change of variable we have transformed the free boundary problem into a fixed boundary. A kind of MLPG method based on the moving least squares approximation, has been applied to solve the direct problem. With an example we tested the direct solver. Inverse problem has been reformulated as a least-squares minimization problem. Computations are performed by *fmincon* routine MATLAB toolbox with the *Interior – point* algorithm. Obtained numerical results are shown that the propose method is accurate and stable, although under a large measurement noise in input data.

Acknowledgements

We thank the anonymous reviewers for helpful comments, which lead to definite improvement in the manuscript.

References

- [1] S. Abbasbandy, H. R. Ghehsareh, I. Hashim, Numerical analysis of a mathematical model for capillary formation in tumor angiogenesis using a meshfree method based on the radial basis function, *Eng. Anal. Boundary. Elem.* 36(12) (2012) 1811–1818.
- [2] S. Abbasbandy, H. R. Ghehsareh, I. Hashim, A meshfree method for the solution of two-dimensional cubic nonlinear Schrödinger equation, *Eng. Anal. Boundary. Elem.* 37(6) (2013) 885–898.
- [3] S. Abbasbandy, A. Shirzadi, MLPG method for two-dimensional diffusion equation with Neumann's and non-classical boundary conditions, *Appl. Numer. Math.* 61 (2011) 170–180.
- [4] S. N. Atluri, *The Meshless Method (MLPG) for Domain and BIE Discretizations*, Tech Science Press, Amazon, 2004.
- [5] S. N. Atluri, S. P. Shen, The meshless local Petrov-Galerkin (MLPG) method: A simple and less-costly alternative to the finite element methods, *Comput. Model. Eng. Sci.* 3(1) (2002) 11–51.
- [6] S. N. Atluri, T. Zhu, A new meshless local Petrov-Galerkin (MLPG) approach in computational mechanics, *Comput. Mech.* 22(2) (1998) 117–127.
- [7] S. N. Atluri, T. Zhu, A new meshless local Petrov-Galerkin (MLPG) approach to nonlinear problems in computer modeling and simulation, *Comput. Model. Simul. Eng.* 3(3) (1998) 187–196.
- [8] S. N. Atluri, T. Zhu, The meshless local Petrov-Galerkin (MLPG) approach for solving problems in elasto-statics, *Comput. Mech.* 25 (2000) 169–179.
- [9] S. N. Atluri, T. Zhu, New concepts in meshless methods, *Int. J. Numer. Meth. Eng.* 13 (2000) 537–556.
- [10] F. Bai, D. Li, J. Wang, Y. Cheng, An improved complex variable element-free Galerkin method for two-dimensional elasticity problems, *Chin. Phys B* 21 (2012) 020204–1–020204–10.
- [11] T. Belytschko, Y. Y. Lu, L. Gu, Element-free Galerkin methods, *Int. J. Numer. Methods Eng.* 37(2) (1994) 229–256.
- [12] T. Belytschko, Y. Y. Lu, L. Gu, Element free Galerkin methods for static and dynamic fracture, *Int. J. Solids Struct.* 32 (1995) 2547–2570.
- [13] J. Cannon, *The One-dimensional Heat Equation*, Cambridge University Press, Florida, 1984.
- [14] H. Cheng, M. J. Peng, Y. M. Cheng, A fast complex variable element-free Galerkin method for three-dimensional wave propagation problems, *Int. J. Appl. Mech.* 9(6) (2017) 1750090.
- [15] H. Cheng, M. J. Peng, Y. M. Cheng, The dimension splitting and improved complex variable element-free Galerkin method for 3-dimensional transient heat conduction problems, *Int. J. Numer. Methods Eng.* 114(3) (2018) 321–345.
- [16] R. J. Cheng, Y. M. Cheng, The meshless method for a two-dimensional inverse heat conduction problem with a source parameter, *Chinese J. Theoret. Appl. Mech.* 39(6) (2007) 843–847.
- [17] Y. M. Cheng, R. J. Cheng, The meshless method for solving the inverse heat conduction problem with a source parameter, *Acta. Phys. Sin.* 56(10) (2007) 5569–5574.
- [18] J. Crank, *Free and Moving Boundary Problems*, Clarendon Press, Oxford, 1984.
- [19] B. Dai, Y. Cheng, An improved local boundary integral equation method for two-dimensional potential problems, *Int. J. Appl. Mech.* 2 (2010) 421–436.
- [20] M. Dehghan, D. Mirzaei, The meshless local Petrov-Galerkin (MLPG) method for the generalized two-dimensional non-linear Schrödinger equation, *Eng. Anal. Boundary. Elem.* 32 (2008) 747–756.
- [21] M. Dehghan, D. Mirzaei, Meshless local Petrov-Galerkin (MLPG) method for the unsteady magnetohydrodynamic (MHD) flow through pipe with arbitrary wall conductivity, *Appl. Numer. Math.* 59 (2009) 1043–1058.
- [22] M. Dehghan, A. Shokri, A numerical method for solution of the two dimensional sine-Gordon equation using the radial basis functions, *Math. Comput. Simul.* 79 (2008) 700–715.
- [23] R. Grzymkowski, D. Slota, Stefan problem solved by Adomian decomposition method, *Int. J. Comput. Math.* 82 (2005) 851–856.
- [24] R. Grzymkowski, D. Slota, One-phase inverse Stefan problem solved by Adomian decomposition method, *Comput. Math. Appl.* 51 (2006) 33–40.
- [25] Y. T. Gu, G. R. Liu, A meshless local Petrov-Galerkin (MLPG) method for free and forced vibration analyses for solids, *Comput. Mech.* 27 (2001) 188–198.
- [26] S. C. Gupta, *The Classical Stefan Problem. Basic Concepts, Modelling and Analysis*, Elsevier, Amsterdam, 2003.
- [27] E. Hetmaniok, D. Slota, R. Witula, A. Zielonka, The solution of one-phase inverse Stefan problem by homotopy analysis method, *Appl. Math. Model.* 39 (2015) 6793–6805.
- [28] M. J. Huntul, D. Lesnic, Determination of a time-dependent free boundary in a two-dimensional parabolic problem, *Int. J. Appl. Comput. Math.* 5 (2019) 118.
- [29] M. Hussein, D. Lesnic, M. Ivancho, H. Snitko, Multiple time-dependent coefficient identification thermal problems with a free boundary, *App. Numer. Math.* 99 (2016) 24–50.
- [30] M. S. Hussein, D. Lesnic, Determination of a time-dependent thermal diffusivity and free boundary in heat conduction, *Int. Commun. Heat Mass Transf.* 53 (2014) 154–163.
- [31] M. S. Hussein, D. Lesnic, M. I. Ivancho, Free boundary determination in nonlinear diffusion, *East Asian J. Appl. Math.* 3 (2013) 295–310.
- [32] M. I. Ivancho, Inverse problem with free boundary for heat equation, *Ukr. Math. J.* 55 (2003) 1086–1098.
- [33] B. T. Johansson, D. Lesnic, T. Reeve, A method of fundamental solutions for the one-dimensional inverse Stefan problem, *Appl. Math. Model. Simul. Comput. Eng. Environmental Syst.* 35 (2011) 4367–4378.
- [34] E. Kansa, Multiquadrics-a scattered data approximation scheme with applications to computational fluid-dynamics. I. surface approximations and partial derivative estimates, *Comput. Math. Appl.* 19(8-9) (1990) 127–145.
- [35] A. Karami, S. Abbasbandy, E. Shivanian, Meshless local Petrov Galerkin formulation of inverse Stefan problem via moving least squares approximation, *Math. Comput. Appl.* 24 (2019) 101.

- [36] C. S. Liu, Solving two typical inverse Stefan problems by using the Lie-group shooting method, *Int. J. Heat and Mass Transfer*. 54 (2011) 1941–1949.
- [37] F. B. Liu, Y. M. Cheng, The improved element-free Galerkin method based on the nonsingular weight functions for inhomogeneous swelling of polymer gels, *Int. J. Appl. Mech.* 10(4) (2018) 1850047.
- [38] F. B. Liu, Q. N. Wu, Y. M. Cheng, A meshless method based on the nonsingular weight functions for elastoplastic large deformation problems, *Int. J. Appl. Mech.* 11(1) (2019) 1950006.
- [39] G. R. Liu, Y. T. Gu, *An Introduction to Meshfree Methods and Their Programming*, Springer, 2005.
- [40] Y. Lotfi, K. Parand, K. Rashedi, J. AmaniRad, Numerical study of temperature distribution in an inverse moving boundary problem using a meshless method, *Engineering with Computers*. 35 (2019) 1–15.
- [41] A. Meirmanov, *The Stefan Problem*, Walter de Gruyter, Berlin, 1992.
- [42] O. N. Onyejekwe, The solution of one-phase inverse Stefan problem by homotopy analysis method, *Appl. Math. Sci.* 8 (2014) 2635–2644.
- [43] M. N. Ozisik, *Heat Conduction*, Wiley, New York, 1980.
- [44] M. Peng, D. Li, Y. Cheng, The complex variable element-free Galerkin (CVEFG) method for elasto-plasticity problems, *Eng Struct* 33 (2011) 127–135.
- [45] M. J. Peng, P. Liu, Y. M. Cheng, The complex variable element-free Galerkin (CVEFG) method for two-dimensional elasticity problems, *Int. J. Appl. Mech.* 1(2) (2009) 367–385.
- [46] H. P. Ren, Y. M. Cheng, The interpolating element-free Galerkin (IEFG) method for two-dimensional potential problems, *Eng. Anal. Boundary. Elem.* 36 (2012) 873–880.
- [47] L. I. Rubinstein, *The Stefan Problem*, AMS, Providence, 1971.
- [48] E. Shivanian, H. H. Alsulami, M. S. Alhuthali, S. Abbasbandy, Predictor homotopy analysis method (PHAM) for nano boundary layer flows with nonlinear Navier boundary condition: existence of four solutions, *Filomat* 28 (2014) 1687–1697.
- [49] J. Sladek, V. Sladek, Y. C. Hon, Inverse heat conduction problems by meshless local Petrov Galerkin method, *Eng. Anal. Boundary. Elem.* 30 (2006) 650–661.
- [50] J. Sladek, V. Sladek, P. Wen, Y. Hon, The inverse problem of determining heat transfer coefficients by the meshless local Petrov Galerkin method, *Comput. Model. Eng. Sci.* 48 (2009) 20–32.
- [51] D. Slota, Direct and inverse one-phase Stefan problem solved by the variational iteration method, *Comput. Math. Appl.* 54 (2007) 1139–1146.
- [52] D. Slota, The application of the homotopy perturbation method to one-phase inverse Stefan problem, *Int. J. Comput. Math.* 37 (2010) 587–592.
- [53] Y. J. Weng, Z. Zhang, Y. M. Cheng, The complex variable reproducing kernel particle method for two-dimensional inverse heat conduction problems, *Eng. Anal. Boundary. Elem.* 44 (2014) 36–44.
- [54] L. Xiaolin, L. Lishuling, Analysis of the complex moving least squares approximation and the associated element-free Galerkin methods, *Appl. Math. Model.* 47 (2017) 45–62.
- [55] S. Y. Yu, M. J. Peng, H. Cheng, Y. M. Cheng, The improved element-free Galerkin method for three-dimensional elastoplasticity problems, *Eng. Anal. Boundary. Elem.* 104 (2019) 215–224.
- [56] N. Zabararas, Y. Ruan, A deforming finite element method analysis of inverse Stefan problems, *Int. J. for Numer. Meth. Eng.* 28 (1989) 295–313.
- [57] T. Zhang, Y. He, L. Dong, S. Li, A. Alotaibi, S. N. Atluri, Meshless local Petrov-Galerkin mixed collocation method for solving Cauchy inverse problems of steady-state heat transfer, *Comput. Model. Eng. Sci.* 97 (2014) 509–533.
- [58] Z. Zhang, S. Hao, K. Liew, Y. Cheng, The improved element-free Galerkin method for two-dimensional elastodynamics problems, *Eng. Anal. Boundary. Elem.* 37(12) (2013) 1576–1584.
- [59] Z. Zhang, D. Li, Y. Cheng, K. Liew, The improved element-free Galerkin method for three-dimensional wave equation, *Acta Mech. Sin.* 28 (2012) 808–818.